Journal of Molecular Catalysis B: Enzymatic 102 (2014) 72–80

Contents lists available at ScienceDirect

Journal of Molecular Catalysis B: Enzymatic

journal homepage: www.elsevier.com/locate/molcatb

Novel hybrid materials on the basis of nanostructured tin dioxide and a lipase from *Rhizopus delemar* with improved enantioselectivity

Maya Guncheva[a,*], Momtchil Dimitrov[a], François Napoly[b], Micheline Draye[c], Bruno Andrioletti[b]

[a] Institute of Organic Chemistry with Centre of Phytochemistry, Bulgarian Academy of Sciences, 1113 Sofia, Bulgaria
[b] Institut de Chimie et Biochimie Moléculaires et Supramoléculaire (ICBMS-UMR CNRS 5246), Université Claude Bernard Lyon1, Bâtiment Curien (CPE), 43, Bd du 11 Novembre 1918, 69622-Villeurbanne-cedex, France
[c] Laboratoire de Chimie Moléculaire et Environnement, Université de Savoie, CISM, Campus Scientifique, 73376 Le Bourget du Lac Cedex, France

ARTICLE INFO

Article history:
Received 12 October 2013
Received in revised form 27 January 2014
Accepted 27 January 2014
Available online 4 February 2014

Keywords:
Amino-functionalized nanosized tin dioxide
Rhizopus delemar lipase
Pyrrolidinium -based ionic liquids
Enantioselectivity

ABSTRACT

We obtained novel hybrid materials on the basis of covalently bounded to amino-grafted tin dioxide lipase from *Rhizopus delemar* (NH_2-nano-SnO_2-RhD). Under the optimal condition, the protein loading yielded of 14.7 mg/g NH_2-nano-SnO_2, while the adsorption capacity of the unmodified nano-SnO_2 for the same enzyme was 38.5 mg/g. At the same time, NH_2-nano-SnO_2-RhD exhibited specific hydrolytic activity of 77.6 U/mg prot. which is 2.5-fold higher in comparison to that of the physically adsorbed on nano-SnO_2 lipase (nano-SnO_2-RhD). In ten reaction cycles of tributyrin hydrolysis, up to 70% of the activity of NH_2-nano-SnO_2-RhD was preserved. Upon immobilization the enantioselectivity of the lipase for the reaction of acylation of (±)-menthol was improved. For the two biocatalysts, the highest yield of (−)-menthyl acetate (more than 35%) was obtained when glyceryl triacetate was used as acylating reagent, however, the enantiomeric excess was only 89.5% for the covalently bonded lipase and 85.0% for the physically adsorbed one. Higher enantiomeric excess was obtained when vinyl acetate was used as an acylating reagent; however, the conversion in that case did not exceed 20%. The addition of small amounts of pyrrolidinium-based ionic liquids, 1-methyl-1-octyl-pyrrolidinium bis(trifluoromethyl)sulfonyl imide [MOPyrro][NTf_2], 1-methyl-1-octyl-pyrrolidinium hexafluorophosphate [MOPyrro][PF_6], and 1-methyl-1-octyl-pyrrolidinium tetrafluoroborate [MOPyrro][BF_4], to the reaction mixture resulted in decrease of (±) menthol conversion rate. All tested ionic liquids enhanced the enantioselectivity of nano-SnO2-RhD, and the best result was obtained in presence of [MOPyrro][PF6] (enantiomeric ratio >140).

1. Introduction

Lipases (triacylglycerol acylhydrolase, EC 3.1.1.3) are large group of enzymes that catalyze hydrolysis of ester-bonds in triglyceride substrates to glycerol and free fatty acids. They also can catalyze the reversed reaction of esterification in non-aqueous medium. Their catalytic centre consists of a triad of amino acid residues (serine, histidine, and aspartate or glutamate), which realize the nucleophilic attack of the carbonyl carbon atom of the scissile ester bond. In the due course of the catalytic reaction, tetrahedral intermediate is formed and is stabilized by hydrogen bonding with amino acid residues of the so-called "oxyanion hole" [1]. General feature of the most of lipases is the existence of α-helical loop that covers the active site. The lid undergoes conformational change in presence of water-lipid interface, moves away and makes the active centre accessible for the substrate molecules. The phenomenon is called interfacial activation; it is common for lipases and distinguishes them from esterases [2,3]. Some of the lipases exhibited broad substrate specificity. On the contrary, other lipases demonstrated preferences in respect to the chain-length or number of double bonds of the fatty acid moieties and/or position of the scissile ester bond in the glycerol skeleton of the substrates. According to enzyme database thousands of lipases of bacterial, mammalian and plant origin have been isolated and preliminary characterized up to date. Special attention has been focused on microbial lipases due to their easy production, good stability, and versatile applicability. They are widely used in food, detergent, textile, paper, pharmaceutical industries, in medicine as a diagnostic tool, *etc.* [4,5]. Recent studies have shown that lipases can also successfully catalyse aldol reactions, Michael and aza-Markovnicov addition reactions, Mannich reactions, ring-opening polymerization, *etc.* in laboratory scale [6–8]. This reveals their novel potential application in fine organic synthesis.

* Corresponding author. Tel.: +359 29606160; fax: +359 2 8700 225.
E-mail address: maiag@orgchm.bas.bg (M. Guncheva).

1381-1177/$ – see front matter © 2014 Elsevier B.V. All rights reserved.
http://dx.doi.org/10.1016/j.molcatb.2014.01.017

Biocatalysts have many advantages over conventional catalysts such as: higher selectivity, non-toxicity, and water-solubility. Furthermore, enzymes are highly active under mild reaction conditions, and their use reduces both energy consumption and environmental pollution. However, their large scale utilization is still limited due to their high price and low stability in harsh reaction conditions. Therefore, lipase stabilization and possibility for their application in multiple runs have been in the focus of many studies. The most effective approaches to enhance and preserve the activity of biocatalysts are enzyme immobilization and media engineering. For example, a remarkable hyperactivation (up to 2000-fold) in respect to the soluble enzyme has been reported for several lipases immobilized on octyl-agarose [9]. Outstanding heat and storage stability, solvent tolerance and multiple reuses have been reported for many immobilized lipases from various spices [10–12]. In combination with immobilization, lipase exploitation in non-conventional medium (ionic liquids, supercritical carbon dioxide, liquid polymers, fluorous solvents, high/low pressure) may significantly enhance reaction rate and enhance or alter enzyme enantioselectivity [13].

Novel cheap inorganic materials with high specific area and good physical and mechanical stability for enzyme carriers are still of demand. In contrast to organic polymer and biopolymer materials, such carriers are resistant to microbial attack, solvents and oils. Inorganic materials with morphological features on the nano-scale have high outer surface which is a prerequisite for high protein loadings on the external surface and hence one serious problem typical for mesoporous carriers as diffusion limitation can be overcome. In many cases, porous materials ensure appropriate microenvironment for enzyme and seem to provide better stabilization of protein molecules than their non-porous counterparts [14].

Our previous studies have shown that upon immobilization on nanosized tin dioxide lipases from *Rhizopus delemar* and *Candida rugosa* were not only stabilized but also activated in comparison with the same biocatalysts adsorbed on polypropylene or mesoporous silica [15,16]. However, the low protein loading obtained on the nanosized tin dioxide was a significant drawback. This novel material has not been fully explored as enzyme carrier and the favorable results motivate further optimization of both the support and the immobilization procedure.

In general, amino-grafted inorganic materials are very suitable for covalent bonding of enzymes and a serious problem with enzyme leakage, common to physically adsorbed proteins, can be avoided. For example, remarkable results with amino-modified supports in terms of protein loading and activity have been reported for industrially important biocatalysts such as: invertases, lipases, proteases, and other enzymes [17–19].

Hence, we aim to prepare novel amino-functionalized nanosized tin dioxide, and to test the effect of the modification of the material on its lipase immobilization efficiency. Furthermore, amino-functionalized inorganic materials are valuable materials due to their various applications. They are used as adsorbents for toxic compounds, CO_2, *etc.* [20,21], amino-grafted silica, for example, was found to be effective base catalysts for Knovenagel condensation and Michael addition reactions [22,23]. Furthermore, functionalized silica nanoparticles have been extensively studied in view of their applicability for cell labelling, magnetic resonance imaging, controlled drug delivery, *etc.* [24].

In this paper we describe the synthesis of novel amino-grafted nanosized tin dioxide (NH_2-nano-SnO_2). We applied the material for covalent bonding of a lipase from *R. delemar*, industrially important 1, 3-specific enzyme widely used for production of structured lipids for clinical nutrition, infant formulas and other high-value lipids like cocoa butter analogue using widespread and inexpensive fats [25–27]. The enzyme is monomer with molecular weight 30.3 kDa and displays "interfacial activation" upon contact with hydrophobic surfaces [28]. We tested both hydrolytic and synthetic activity of the novel biocatalyst. The enantioselectivity of the enzyme preparation was estimated in reaction of kinetic resolution of (±)-menthol and for this reaction the effect of the temperature, acyl donor and reaction medium was followed. All results are discussed in comparison with those obtained for physically adsorbed on nanosized tin dioxide *R. delemar lipase*.

2. Experimental

2.1. Materials

Lipase from *R. delemar* (RhD) (lyophilized powder, 20% protein content, 100 U/mg, olive oil as substrate) was purchased from Kerry Bio-Science and was used without purification. Glyceryl tributyrate (99%), Folin & Ciocalteu's phenol reagent (2 N, suitable for determination of total protein by Lowry's method), (±)-menthol (98%), (1R,2S,5R) (−)-menthol (99%), (1S, 2R, 5S)(+)-menthol (99%), vinyl acetate (> 99%), glutaraldehyde solution, grade II, 25% in H_2O, tin (IV) chloride (>99.9% purity), (3-aminopropyl)triethoxysilane (APTES), and Pluronic 123 (M_W 5800) were purchased from Sigma–Aldrich. Acetic anhydride (>99%) and glyceryl triacetate (triacetin) (>99%) were obtained from Fluka. 1-methylpyrrolidine, 1-octylbromide, KPF_6 and $NaBF_4$ were purchased from ACROS. LiNTf2 was obtained from Solvionic. Standards of (−)-menthyl acetate and (+)-menthyl acetate were synthesized according to literature procedure [29]. The synthesis of 1-methyl-1-octyl-pyrrolidinium bis(trifluoromethyl)sulfonyl imide [MOPyrro][NTf_2], 1-methyl-1-octyl-pyrrolidinium hexafluorophosphate [MOPyrro][PF_6], and 1-methyl-1-octyl-pyrrolidinium tetrafluoroborate [MOPyrro][BF_4] is described in Section 2.4. Analytical grade solvents were purchased from Labscan.

2.2. Synthesis of the nanosized tin dioxide

The synthesis of the nanostructured SnO_2 material was conducted by controlled hydrolysis of $SnCl_4$ in the presence of ethanol, water and block copolymer (Pluronic P123) as described previously [30]. In short, 3.00 g of $SnCl_4$ were added to a solution of 4.15 g distilled water, 26.53 g ethanol, and 1.45 g Pluronic P123 as a surfactant, and a sol with the following molar compositions was obtained: 1.00 $SnCl_4$:0.01 P123:50 ethanol:20.00 H_2O

The as-prepared sol was stirred for 4 h at 313 K and then the solvent was removed in a rotary evaporator at 313 K. The obtained material was freeze-dried overnight and finally calcined using a stepwise procedure with a temperature increase of 1 K/min up to 573 K and dwelling times of 6 h at 373 K, 4 h at 423 K, 4 h at 473, 4 h at 523 and 4 h at 573 K. The obtained pure tin dioxide powder was designated as nano-SnO_2.

The amino-functionalization of nano-SnO_2 was carried out with 3-aminopropyltriethoxysilane (APTES). To graft the support surface, APTES (3.6 mmol/g) has been added to 100 mL ethanol containing 1 g nano-SnO_2 (activated for 2 h at 423 K for physisorbed water removal) and the mixture was stirred for 5 h at 323 K followed by filtration with ethanol and drying at room temperature. The amino-functionalized material was designated as NH_2-nano-SnO_2.

2.3. Characterization of the particles

Powder X-ray diffraction patterns were collected within the range of 20–80° 2θ with a constant step of 0.02° 2θ and counting time of 1 s/step on Bruker D8 Advance diffractometer equipped with Cu Kα radiation and LynxEye detector. The size of the crystalline domains in the samples was determined based on the

Scherrer equation [31], using the line broadening of the 110 Bragg reflection (the fitting of the diffraction patterns was carried out with Lorentzian peak function). Nitrogen sorption measurements were recorded on a Belsorp- mini II (BEL Japan) at 77 K. Before the physisorption measurements the samples were outgassed at 423 K overnight under vacuum. Thermogravimetric analysis was conducted on a Setaram TGA 92 instrument, in order to follow the changes with the obtained support materials with temperature increase in air up to 600 °C and a ramp of 5 °C/min.

The amount of the amino groups in NH_2-nano-SnO_2 samples was determined by ninhydrin test according to the procedure described by Soto-Cantu et al. [32]. Octylamine was used in order to build the calibration plot.

2.4. Preparation of ionic liquids

The ionic liquids were prepared according to the optimized procedure reported by Chatel et al. [33]. In a typical reaction, 1.2 eq. of 1-methylpyrrolidine was reacted with 1 eq. of 1-bromooctane in ethyl acetate (5.6 eq.) under Argon. The reaction mixture was brought to reflux and heated for 24 h. The resulting white suspension was filtered off and the solid was washed twice with ethyl acetate. The solid was transferred in a round bottom flask and dissolved in methanol. Methanol was evaporated under vacuum affording a hygroscopic white powder in 90% yield.

2.4.1. Anion metathesis

The bromo-pyrrolidinium obtained above was solubilized in distilled water (1:2, w/w) and the appropriate counter anion salt ($LiNTf_2$, KPF_6 or $NABF_4$) was added (1 eq.) under Argon. The reaction mixture was allowed to stir at room temperature for 12 h. Then, the reaction mixture was extracted 3 times with dichloromethane. The combined organic phases were washed with H_2O, dried over $MgSO_4$, filtered and treated with charcoal for 2 h. Charcoal was removed by filtation over celite, and the filtrate was evaporated *in vacuo* affording pale yellow ionic liquids in 63–93% yield.

2.4.2. Typical NMR data for (MOPyrro)NTf_2

^{1}H NMR (δ ppm, $CDCl_3$, 300 MHz): δ 3.57 (4H, m, N–CH_2), 3.37 (2H, m, N–CH_2), 3.06 (3H, s, N–CH_3), 2.21 (4H, m, 2CH_2), 1.76–1.65 (2H, m, CH_2), 1.33–1.20 (10H, m, 5CH_2), 0.82 (3H, t, J = 6.7 Hz, CH_3).

^{13}C NMR (δ ppm, $CDCl_3$, 75 MHz): δ 119.7, 64.1, 63.9, 47.7, 31.0, 28.3 (2C), 25.6, 23.2, 21.9 (2C), 20.8 (2C), 13.4.

2.5. Immobilization of lipase from Rhizopus delemar

We prepared solutions of *R. delemar* lipase in 0.05 M sodium phosphate buffer (pH 7.3) with lipase concentrations varying in the range from 0.5 mg/mL to 5 mg/mL (20% protein content). The immobilization experiments were carried out by mixing 50 mg of nanosized tin dioxide with 10 mL lipase solution (*i.e.* protein loadings 10.0–100.0 mg/g carrier), and the mixture was magnetically stirred for 12 h at room temperature. Then, the biocatalysts were filtered, rinsed with 2 mL sodium phosphate buffer, and dried under nitrogen.

The nano-SnO_2 was used without any pre-treatment while prior to use NH_2-nano-SnO_2 was modified with glutaraldehyde. Generally, 10 mL glutaraldehyde solution (25%) was added to a suspension of 2.00 g NH_2-nano-SnO_2 in 50 mL sodium phosphate buffer (pH 7.3, 0.05 M). The mixture was magnetically stirred at room temperature for 2 h, then the modified NH_2-nano-SnO_2 was rinsed consequently with two portions of 10 mL sodium phosphate buffer (pH 7.3, 0.05 M), and distilled water.

The amount of the protein immobilized on the carrier (mg protein/g support) was calculated by the following equation:

$$Q_e = \frac{V(C_o - C_e)}{m},$$

where C_0 and C_e (mg/mL) are the initial and the final protein concentration of the lipase loading solutions, respectively, V (mL) is the volume of the enzyme solution, m (g) is the quantity of the support. The Langmuir and Freundlich constants were calculated as described in the literature [34].

2.6. Protein assay

The amount of the protein in the enzyme solutions was estimated according to Lowry's method using bovine serum albumin as standard [35]. The amount of immobilized protein was calculated from the difference between the protein content in the initial enzyme solution and the supernatant after the immobilization.

2.7. Hydrolytic activity assay

The hydrolytic activity of the biocatalysts was assessed titrimetrically using 0.05 M sodium hydroxide as titrant. Initially, 0.1 mL tributyrin, 0.5 mg gum arabica, and 5 mL sodium phosphate buffer (50 mM, pH 7.0) were kept at 40 °C for 5 min, then 1-2 mg immobilized enzyme (or 20 μL free lipase with concentration of 8 mg/mL) were added. The reaction was performed for 20 min at 40 °C under gentle stirring, and then was terminated by adding 5 mL mixture of ethanol and acetone (1:1, v/v).

The effect of the ILs on the hydrolytic activity of the immobilized lipase from *R. delemar* was estimated using the above described procedure in presence of 10 mmol of each pyrrolidinium-based salt.

The spontaneous hydrolysis was taken into consideration and control parallel non-enzymatic reaction (without and with ILs) was run. One lipase unit (U) is defined as the amount of enzyme required to liberate 1 μmol butyric acid per min under the assay conditions. The activity of the immobilized lipase preparations is presented as the number of lipase units per gram support (U/g carrier). The specific activity corresponds to the number of lipase units per mg of protein (U/mg prot.).

To test the stability of the immobilized lipase from *R. delemar* in several consecutive cycles after each batch reaction, the biocatalyst was recovered by filtration, washed with 1 mL of dry hexane, and added to the fresh substrate mixture without other treatment. The activity of the immobilized enzyme in the first cycle was taken for 100% and the relative activity for the following cycles was calculated with respect to it.

2.8. Kinetic resolution of menthol

In a typical experiment, 4 mmol of (±)-menthol and 5U biocatalyst were added to 1 mL hexane in a screw-capped vial. The reaction was initiated by adding 4 mmol acylating reagent (vinyl acetate). The reaction mixture was magnetically stirred (200 rpm) at 25 °C for 20 h. The initial water activity of the reaction mixture was maintained at 0.33 by using saturated solution of magnesium chloride [36], and then maintained using molecular sieve 3 Å. Control experiments without enzyme were performed. To determine the temperature effect on the efficiency and enantioselectivity of both studied biocatalysts, the reactions of acylation of (±)-menthol with vinylacetate were performed in the temperature range from 20 °C to 40 °C. To determine the effect of ionic liquids on the enantioselectivity of nano-SnO_2-RhD and NH_2-nano-SnO_2-RhD, 1 mmol of IL were added to the reaction mixtures.

Aliquots (100 μL) from the reaction mixture were withdrawn periodically, extracted with 500 μL of hexane/5%$NaHCO_3$ (1:1), and

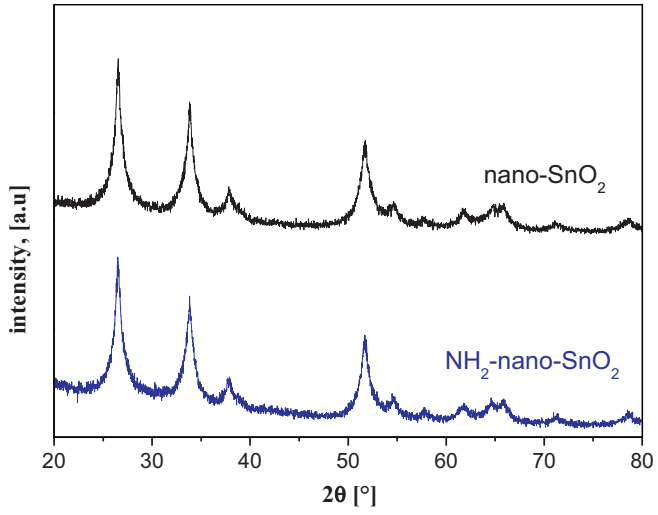

Fig. 1. X-ray diffraction patterns of pure and functionalized nanosized tin dioxide.

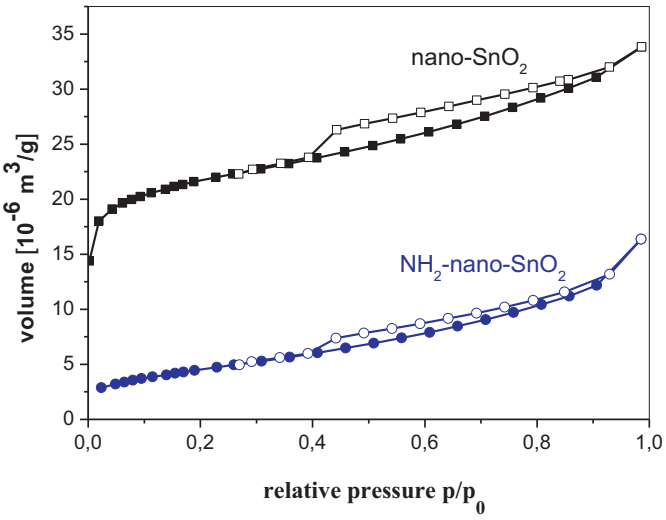

Fig. 2. Nitrogen physisorption isotherms of pure and functionalized nanosized tin dioxide.

the hexane layer was analyzed by gas chromatography. The analyses were performed on a Shimadzu GC-17A instrument equipped with CycloSil-B (Agilent) column (0.25 μm × 0.25 mm × 30 m) and fitted with a flame ionization detector. The column was maintained at 90 °C for 10 min, and then the temperature was increased first to 150 °C at 3 °C/min, and after that to 165 °C at 5 °C/min, and finally the temperature was maintained at 165 °C for 5 min. The temperature of the injector was 220 °C and that of the detector −250 °C. Nitrogen was used as a gas carrier. The retention times were 24.3 min for (+)-menthol, 25.1 min for (−)-menthol, 33.5 min for (−)-menthyl acetate, and 34.1 min for (+)-menthyl acetate.

The conversion in percentage was calculated from the following equation:

$$c = \left(1 - \frac{S}{S_0}\right) \times 100,$$

where S_0 and S stand for the concentration of (±)-menthol at the beginning and at the end of the reaction, respectively.

The enantioselectivity for each reaction was expressed by enantiomeric excess (e.e.(P_-)) and enantiomeric ratio (E-value), which was calculated using the equation given by Straathof and Jongejan [37].

$$\text{e.e.}(P_-)(\%) = \frac{P_- - P_+}{P_- + P_+} \times 100$$

$E = \frac{\ln(1-c(1+\text{e.e.}P_-))}{\ln(1-c(1-\text{e.e.}P_-))}$, where P_- and P_+ represent the ratios of (−)-menthyl acetate and (+)-menthyl acetate to total menthyl acetate, respectively.

2.9. Statistical analysis

All experiments were performed in triplicate: the average values were reported along with Standard deviation.

3. Results and discussion

3.1. Characterization of the nanosized materials

Powder X-ray diffraction (PXRD) was applied for the identification of initial SnO_2 crystalline phases (Fig. 1). PXRD patterns of both studied support materials show reflections typical of cassiterite (not shown) with similar particle sizes of about 8.5 nm (Table 1). The pore characteristics of the studied tin dioxide materials were determined by physisorption measurements with nitrogen at 77 K (Fig. 2, Table 1). The obtained isotherms can be classified as type IV isotherms according to IUPAC classification, which is characteristic of mesoporous materials with high energies of adsorption and often contain hysteresis loops usually associated with capillary condensation in the mesoporous structure. For both samples, the found gradual increase of the adsorption branch of their isotherms could be assigned to a broad pore size distribution with a predominant presence of pores due to interparticle mesoporosity. The obtained hysteresis could be defined as inverse type H2 loop associated with the occurrence of pore blocking [38]. In this case the desorption branch is less steep than the adsorption branch. Such a hysteresis could be observed in materials where the pore size distribution of the main pores is narrower than the pore size distribution of the entrance diameters. The initial nano-SnO_2 material possesses high specific surface area due to particle and pore sizes in the nanoscale (Table 1). This is the first report on amino-functionalization of nanosized tin dioxide. The grafting with 3-aminopropyltriethoxysilane (APTES) provokes some changes in the support characteristics, a substantial decrease in BET surface area and pore volume as well as changes in the mean pore diameter that we assign to blocking of the pores of the support and the outer surface by the APTES molecules (Fig. 1, Table 1). Besides, during the conducted thermogravimetric experiments in air up to 600 °C of the studied supports (Fig. 3), the

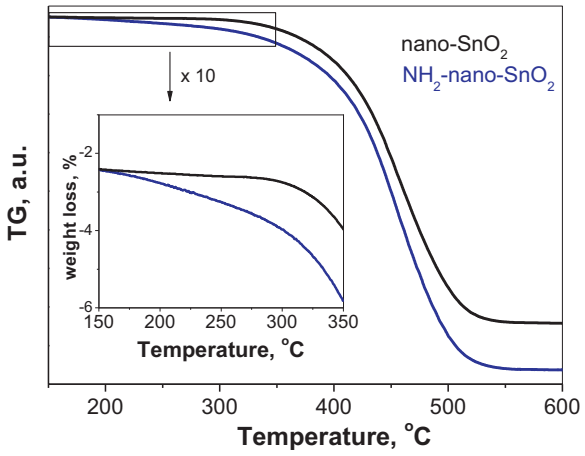

Fig. 3. Thermogravimetric analysis of pure and functionalized nanosized tin dioxide conducted in air up to 600 °C.

Table 1
Textural characteristics of the materials.

Sample	Textural characteristics of the tin dioxides			
	Surface area, m^2/g	Total pore volume, cm^3/g	Mean pore diameter, nm	Particle size, nm
Nano-SnO_2	79.3	0.052	2.6	8.4
NH_2-nano-SnO_2	16.1	0.025	6.3	8.6

observed mass loss in the temperature range of 200–300 °C registered only for NH_2-nano-SnO_2, which we ascribe to decomposition of the grafted APTES molecules. The result is in accordance with that observed from physisorption experiments and confirms that the grafting was successful. The registered considerable weight loss for both samples at temperatures above 300 °C is due to processes of agglomeration of the small SnO_2 nanoparticles. Using spectrophotometric assay [32], we estimated that for NH_2-nano-SnO_2 samples the density of amino groups is 3.0 mmol/g, which is up to three fold higher than the amount of the same groups reported in the literature for aminopropyl modified mesoporous silica with significantly higher surface area [22,24].

3.2. Immobilization of Rhizopus delemar lipase

In the literature there are scarce data on the immobilization of *R. delemar* lipase. Most of the papers related to this enzyme are focused on its application and the immobilization procedures were performed by analogy to the procedures applied to different lipases without optimization. We employed two different immobilization methods for the two synthesized nanosized carriers. We optimized the immobilization procedures with respect to the lipase concentration in the loading solutions. The lipase from *R. delemar* was physically adsorbed on the unmodified tin dioxide (nano-SnO_2-RhD). While for the amino-functionalized nanosized tin dioxide the glutaraldehyde crosslinking method was applied to obtain covalent bounded enzyme (NH_2-nano-SnO_2-RhD). The experimental adsorption isotherms have similar profiles regardless of the applied immobilization method and the adsorption data seem to follow Freundlich pattern (Fig. 4). The adsorption isotherm constants were estimated for Langmuir and Freundlich models (Table 2).

Nano-SnO_2 has small interparticle porosity (2.6 nm) and the enzyme, comparatively larger by volume (4.4 nm × 4.0 nm × 4.5 nm, PDB ID: 1TIC) [39], is most likely to be located on the outer surface of the material. According to the literature data the isoelectric point of SnO_2 is 4-5 [40] and that of the lipase from *Rhizops delemar* is 8.6 [28]. Thus, we assume that the major driving forces for the immobilization are the strong electrostatic interactions between the enzyme and the carrier which are oppositely charged at pH 7.3 (lipase loading solutions). The Freundlich constant ($1/n$) was around 0.49 which implies that the surface of the nano-SnO_2 is not identical and more than one layer can be formed. The formation of molecule aggregates via strong hydrophobic interactions between two protein molecules is a common feature of most of the bacterial lipases and on the basis of these specific lipase-lipase interactions are developed efficient chromatographic methods for their purification [41]. These interactions, however, may cause loss in enzyme activity due to the hindered access of the substrate to the enzyme active site.

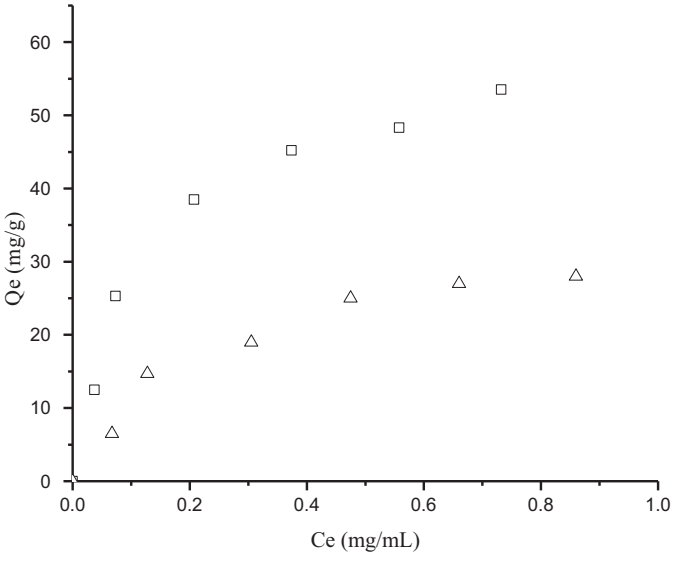

Fig. 4. Adsorption isotherms of lipase from *Rhizopus delemar* on nano-SnO_2 (squares) and NH_2-nano-SnO_2 (triangles).

The addition of small quantities of non ionic detergents to the lipase loading solutions upon immobilization turned out to be a successful approach for monolayer adsorption of lipases from *Pseudomonas fluorescens*, *Thermomyces lanuginosus*, *Aspergilus niger*, *Candida rugiosa*, *Candida antarctica etc.* on various organic polymers [42–44].

There is no literature data for the application of surfactants upon immobilization of lipase from *R. delemar* and for the purpose of comparison we also have not applied this technique in our study. Furthermore, we achieved up to 50% higher protein loading on the nano-SnO_2 than that obtained on nanosized tin dioxide and mesoporous silica with higher surface areas in our earlier study [15].

We observed a typical bell-shaped dependence of lipase specific hydrolytic activity from the quantity of the immobilized enzyme with optimum (31.9 U/mg prot) at loading of 38 mg/g nano-SnO_2. We found that further increase of the amount of the loaded protein on nano-SnO_2 resulted in lower specific activity of the immobilized biocatalyst which can be explained with the multilayer deposition of the lipase molecules.

For the NH_2-nano-SnO_2, the maximum activity (77.6 U/mg prot.) was detected at protein loading of 14.7 mg/g carrier. The protein was tightly anchored to the carrier and we detected no significant enzyme leaching in aqueous medium (<1%). The immobilization yield obtained with this novel carrier is in good agreement with the results described for other lipases bounded on amino-grafted supports via crosslinking with glutaraldehyde. For example, Hwang et al. obtained protein loading of 2.3 mg/g on amino-modified silica for the lipase from *Bacillus stearothermophilus* L1 [45]. Higher yield (18 mg/g) of covalently bound lipase from *Bacillus coagulans* BTS-3 on amino-functionalized nylon-6 was reported in the literature [46].

3.3. Hydrolytic activity and multiple usage of the biocatalysts

Tested in the reaction of hydrolysis of tributyrin, nano-SnO_2-RhD and NH_2-nano-SnO_2-RhD exhibited total activities of the same order of magnitude (1230 U/g carrier and 1141 U/g carrier, respectively). The immobilized biocatalysts demonstrated good activity in presence of small quantities of the tested ionic liquids (substrate: ILs, 10:1 moles). Moreover, the two immobilized biocatalysts exhibited about 70% enhanced relative activity in

Table 2
Langmuir and Freundlich parameters for the immobilization of lipase from *Rhizopus delemar* on nano-SnO_2 and NH_2-nano-RhD.

Lipase from *Rhizopus delemar* on the corresponding carrier	Langmuir isotherm[a]			Freundlich isotherm[b]	
	K_L (mL/g)	aL (mL/mg)	$\frac{K_L}{\alpha_L}$ (mg/g)	K_F (mL/g)	$\frac{1}{n}$
Nano-SnO_2 (physical adsorption)	41.7	0.56	74.1	74.5	0.49
NH_2-nano-SnO_2 (cross-linking)	120.5	2.65	45.5	34.1	0.54

[a] Langmuir constants, the support capacity ($K_{L)}$) and the energy of adsorption a_L are calculated from the linearized equation: $Qe = \frac{K_L \cdot Ce}{1+a_L Ce}$ [34].

[b] Freundlich constants, the support capacity (K_F) and the homogeneity factor ($1/n$) are calculated from the linearized equation: $Q_e = K_F \cdot C_e^{1/n}$ [34].

the reaction medium containing [MOPyrro][PF_6]. The addition of [MOPyrro][NTf_2] or [MOPyrro][BF_4] to the reaction mixture also has positive effect on the physically adsorbed lipase from *R. delemar* and resulted in 20% and 5% higher activity in respect to control reactions without additives. They, however, did not affect the reaction rate of the covalently bounded enzyme.

Utilization of biocatalysts in large scale production is still very expensive. Thus, stable and active immobilized enzyme preparations that are able to perform in several consecutive reaction cycles are on demand. We estimated the reusability of nano-SnO_2-RhD and NH_2-nano-SnO_2-RhD in a reaction of hydrolysis of triglyceride substrate. We observed fast decline in activity of the physically adsorbed *R. delemar* lipase after the first cycle (Fig. 5). This is due to significant leakage (up to 63.5%) of the loaded protein in aqueous reaction medium. In contrast, the covalently bounded enzyme exhibited good stability and up to 70% of its activity was preserved in ten reaction cycles.

3.4. Enantioselectivity of the biocatalysts

We found that the native *R. delemar* exhibited very low activity and did not show selectivity in the reaction of acylation of (±)-menthol which is in agreement with the results obtained by Koshiro et al. [47]. However, the immobilization on the nanosized tin dioxide seemed to stabilize and activate lipase molecules and the reaction rate of the selected reaction was enhanced. The initial choice of the reaction conditions for the enantioselectivity assays with the immobilized lipase preparations was made taking into account the results from the experiments giving preliminary information on their thermal and solvent stability and activity.

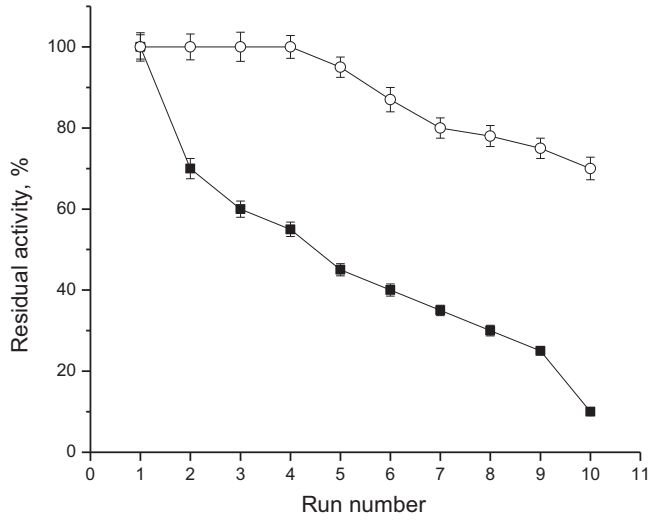

Fig. 5. Operational stability of nano-SnO_2-RhD (close squares) and NH_2-nano-SnO_2-RhD (open circles) in a reaction of tributyrin hydrolysis.

The native enzyme displays the maximal activity at temperatures between 25 and 35 °C. In our previous study, we demonstrated improvement in thermal stability and higher tolerance toward various organic solvents of the immobilized on silica and tin dioxide lipase from *R. delemar* in comparison to the native enzyme [15].

3.4.1. Effect of temperature

In the reaction of hydrolysis of tributyrin, the native enzyme exhibited maximal activity at 40 °C, while shifts in the temperature optimum toward higher temperatures were observed for nano-SnO_2-RhD (50 °C) and NH_2-nano-SnO_2-RhD (45 °C) (data not shown). We assessed the enantioselectivity of the two novel biocatalysts at the temperature range from 20 to 40 °C. Not surprisingly, for the reaction of acylation of (±)-menthol with vinyl acetate in hexane the degree of conversion of substrates increased with an increase of the reaction temperature (Fig. 6). In contrast, the raise of the reaction temperature above the ambient temperature has a negative effect on enantioselectivity of both studied biocatalysts. Therefore, the temperature was maintained at 25 °C for the following experiments.

3.4.2. Effect of the acyl donor

We obtained the highest conversion of (±)-menthol with both biocatalysts when glyceryl triacetate was used as an acyl donor (Table 3). An excellent enantioselectivity ($E > 120$) was obtained with NH_2-nano-SnO_2-RhD when acetic anhydride was used as an acyl donor. However, with this reagent both enzyme preparations were less efficient in terms of substrate conversion. In short time after the beginning of the reaction, we detected significant amount of by-product, which is due to hydrolysis of the acetic anhydride and in this case we attributed the low yields of (−)-menthyl acetate to this side reaction. On the one hand, probably in the anhydrous reaction medium, the anhydride pulls out the water molecules that maintain the enzyme structure, induces conformational change within the protein molecule and inactivates it. On the other hand, the formed short-chain acetic acid may also have an inhibitory effect on the lipase activity. When vinyl acetate was used as an acylating reagent we observed the same degree of conversion for both enzyme preparations but twice higher enantioselectivity for the chemically bounded *R. delemar* lipase. A shift of the reaction equilibrium is expected when vinyl acetate is used as an acyl donor due to irreversible products, vinyl alcohol and acetaldehyde, respectively.

Another possible explanation of the low activity of the free and immobilized lipase from *Rhizopus delmar* in the acylation of cyclic alcohols can be found on the basis of its structure. The substrate binding side of enzyme is shallow and situated near the surface of the enzyme [28] and probably the alcohol can not be accommodated efficiently.

3.4.3. Effect of ILs

We tested the effect of three pyrrolidinium-based ionic liquids (ILs) ([MOPyrro][BF_4], [MOPyrro][PF_6], and [MOPyrro][NTf_2]

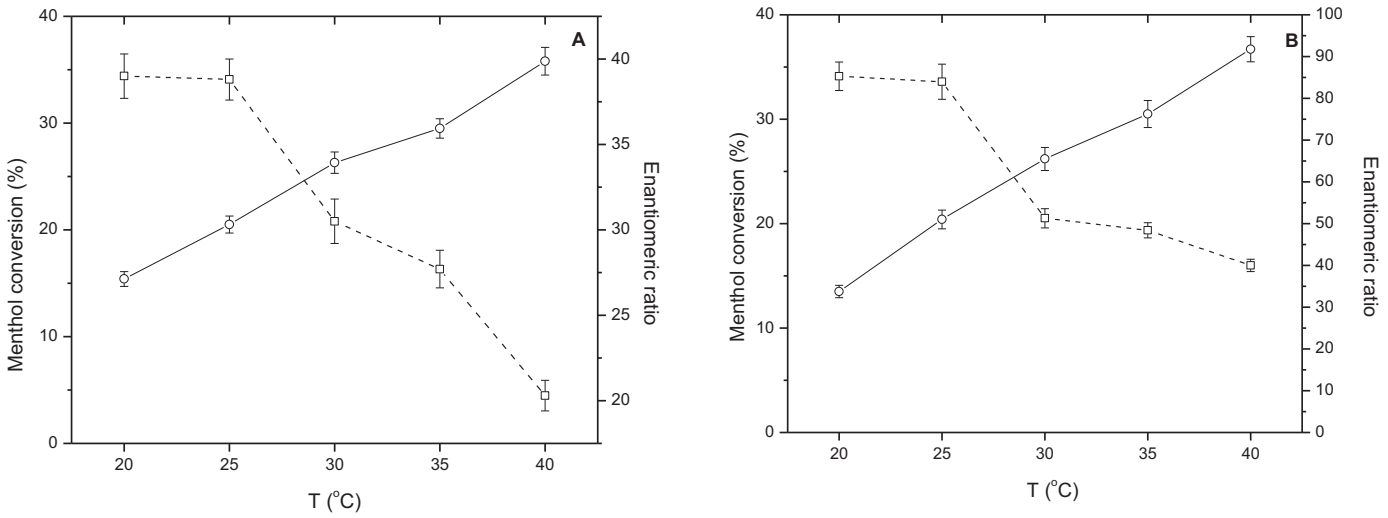

Fig. 6. Effect of temperature on activity and enantioselectivity of the lipase from Rhizopus delemar immobilized on nano-SnO_2 (A) and NH_2-nano-SnO_2 (B) in the reaction of acylation of (±)-menthol.
Reaction conditions: (±-menthol (4 mmol), vinyl acetate (4 mmol) nano-SnO_2-RhD or NH_2-nano-SnO_2-RhD (5U), heating, 200 rpm, 20 h, hexane, aw 0.33.
(±)-menthol conversion (open circle); enantiomeric ratio (open square)

on activity and selectivity of the nano-SnO_2-RhD and NH_2-nano-SnO_2-RhD.

Recently, ionic liquids have been intensively employed as an alternative to organic solvents in enzyme-catalyzed reactions [48]. In some cases, a clear dependence of the enzyme activity from the physico-chemical properties (polarity, viscosity, hydrophobicity) of the ionic liquids was observed but conclusions cannot be generalized yet for all enzymes even those belonging to the same class [49]. In addition, one IL can produce opposite effect on one and the same enzyme applied in two different reactions [50]. Imidazolium based ILs have been most extensively examined reaction media for lipases. For example, Deive et al. clearly demonstrated the excellent extraction properties and stabilization effect of some substituted imidazolium alkyl sulfates on lipases from *C. antarctica* A and *Thermomices lanuginosus* [51,52]. Many lipases have shown higher synthetic activity and enantioselectivity in pure or biphasic system containing 1,3-dialkylimidazolium tetrafluoroborates or 1,3-dialkylimidazolium hexafluorophosphates in comparison to their operation in organic solvents [53–55]. At the same time, for lipases from *Pseudomonas cepacia* and *C. antarctica* B transesterification proceeded more rapidly in 1,3-dialkylimidazolium bis(trifluoromethylsulfonil)amides in comparison to that in other imidazolium based ionic liquids [56,57]. The presence of ILs in the reaction mixture may cause not only change in the enzyme activity but also may alter significantly the enzyme specificity and thus alter the enzyme enantioselectivity. There are scarce data about the influence of pyrrolidinium-based ionic salts on the activity of lipases. Galonde et al. have shown that manosyl myristate synthesis catalyzed by Novozyme 435 proceeded more effectively in N-butyl-N-methylpyrrolidinium trifluoromethane sulfonate [BMPyrro][TFO] than in its imidazolium analogue [BMIM][TFO] [58]. However, the lipase from *C. rugosa* (free and immobilized) did not exhibit activity when was applied in the reaction of transesterification of methyl methacrylate and 2-ethylhexanol in several N-methyl-N-(2-methoxyethyl) pyrrolidinium ionic liquids [48].

For both enzyme preparations, we observed decrease in the rate of menthol conversion in presence of small amounts of the three

Table 3
Effect of >the acyl donor on enantioselectivity of immobilized *Rhizopus delemar* lipase.

Enzyme preparations	Acyl donor (eq.)	Time, h	(±)-Menthol conversion, %	e.e.(P_-), %	Enaniomeric ratio
Nano-SnO_2-RhD	Vinyl acetate (1 eq.)	1	10.3 ± 0.4	93.8	34.5
		20	20.5 ± 0.9	93.6	38.8
	Acetic anhydride (0.5 eq.)	1	6.0 ± 0.2	95.3	44.2
		20	15.7 ± 0.7	95.0	46.3
	Glyceryl triacetate (0.33 eq.)	1	15.2 ± 0.8	87.3	17.2
		20	35.2 ± 1.3	85.0	23.7
NH_2-nano-SnO_2-RhD	Vinyl acetate (1 eq.)	1	8.9 ± 0.4	97.5	85.1
		20	20.4 ± 0.8	97.0	84.0
	Acetic anhydride (0.5 eq.)	1	5.6 ± 0.2	98.3	123.4
		20	19.5 ± 0.8	97.1	85.5
	Glyceryl triacetate (0.33 eq.)	1	13.7 ± 0.5	92.3	28.8
		20	38.5 ± 1.4	89.5	31.7

Reaction conditions: (±)-menthol (4 mmol), acylating reagent (4 mmol), immobilized lipase (5 U), 25 °C, 200 rpm, 20 h, hexane, a_w 0.33.

Table 4
Effect of immobilization of lipase from *Rhizopus delemar* on nanosized tin dioxide (pure and amino-functionalized) on enantioselectivity.

Enzyme preparation	(±) Menthol conversion, %	Enantiomeric excess (P_-), %	Enantiomeric ratio
Native lipase from *Rhizopus delemar*	0.7	–	NA
Nano-SnO_2-RhD	20.5 ± 0.8	93.6	38.8 ± 1.1
+MOPyrroBF_4	9.6 ± 0.4	96.8	67.4 ± 2.6
+MOPyrroNTf_2	8.7 ± 0.3	95.5	47.8 ± 1.8
+MOPyrroPF_6	12.3 ± 0.3	98.4	140.0 ± 5.3
NH_2-nano-SnO_2-RhD	20.4 ± 0.7	97.0	84.0 ± 3.3
+MOPyrroBF_4	7.8 ± 0.2	97.5	80.0 ± 3.6
+MOPyrroNTf_2	7.8 ± 0.2	97.4	85.0 ± 3.5
+MOPyrroPF_6	10.5 ± 0.3	97.3	83.0 ± 3.4

Reaction conditions: (±)menthol (4 mmol), vinyl acetate (4 mmol) and native or immobilized lipase (5 U), 25 °C, 200 rpm, 20 h, hexane, 1 mmol ionic liquid, a_w 0.33.

ionic liquids (Table 4). In the studied reaction, [MOPyrro][BF_4], [MOPyrro][PF_6], and [MOPyrro][NTf_2] did not influence the enantioselectivity of NH_2-nano-SnO_2-RhD preparation as compared to no-additive conditions. In contrast, the physically adsorbed on nano-SnO_2 lipase from *R. delemar* exhibited up to 3.7-fold higher enantioselectivity in presence of ILs. Mohile et al. observed similar effect of imidazolium-based ILs on the *C. rugosa* lipase-catalyzed kinetic resolution of butyl 2-(4-chlorophenoxy) propionate, i.e, decrease in reaction rate and substrate conversion and notable increase in enantioselectivity with increase of the amount of the ILs in the reaction mixture [59]. Similarly, an excellent enantioselectivity ($E > 500$) of immobilized *C. antarctica* B in imidazolium-based ILs in reaction of acylation of 1-phenylethylamine, at very low conversion (5–18%) was reported [60].

4. Conclusions

The synthesized novel hybrid materials on the basis of nanosized tin dioxide and lipase from *R. delemar* demonstrated improved activity and stability than the native enzyme. The two preparations, depending on the reaction conditions, demonstrated moderate to high enantioselectivity in a reaction of acylation of (±)-menthol. The conversion of the target enantiomer exceeded 38% (e.e.(P_-) 89.5%) when glyceryl triacetate was used as an acylating reagent. Although not as good as the results given at the literature for the lipases from *Candida* sp.[61,62], the results in terms of conversion (%) and enantiomeric excess (e.e.(P_-)%) are the best than any previously reported in the literature for *R. delemar* lipase. We estimated that three pyrrolidinium-based ionic liquids have positive effect on the enantioselectivity of the nano-SnO_2-RhD and their interactions with other lipases should be thoroughly examined.

Acknowledgement

The authors thank the National Science Fund of Bulgaria (project DMU 02/20) for the financial support.

References

[1] P. Reis, K. Holmberg, H. Watzke, M. Leser, R. Miller, Adv. Colloid Interface Sci. 147–148 (2009) 237–250.
[2] Z.S. Derewenda, A.M. Sharp, Trends Biochem. Sci. 18 (1993) 20–25.
[3] R. Schmid, R. Verger, Angew. Chem. Int. Ed. 37 (1998) 1608–1633.
[4] F. Hasan, A. Shah, A. Hameed, Enzyme Microb. Technol. 39 (2006) 235–251.
[5] A. Houde, A. Kademi, D. Leblanc, Appl. Biochem. Biotechnol. 118 (2004) 155–170.
[6] M. Kapoor, M. Gupta, Process Biochem. 47 (2012) 555–569.
[7] J.-F. Cai, Z. Guan, Y.-H. He, J. Mol. Catal. B: Enzym. 68 (2011) 240–244.
[8] B. Liu, X. Qian, Q. Wu, X. Lin, Enzyme Microb. Technol. 43 (2008) 375–380.
[9] A. Bastida, P. Sabuquillo, P. Armisen, R. Fernandez-Lafuente, J. Huguet, J. Guisan, Biotechnol. Bioeng. 58 (1998) 486–493.
[10] B. Vaidya, G. Ingavle, S. Ponrathnam, B. Kulkarni, S. Nene, Bioresour. Technol. 99 (2008) 3623–3629.
[11] J. Lu, K. Nie, F. Wang, T. Tan, Bioresour. Technol. 99 (2008) 6070–6074.
[12] N. Ognjanovic, D. Bezbradica, Z. Knezevic-Jugovic, Bioresour. Technol. 100 (2009) 5146–5154.
[13] P. Lozano, Green Chem. 12 (2010) 555–569.
[14] C. Garcia-Galan, A. Berenguer-Murcia, R. Fernandez-Lafuente, R. Rodrigues, Adv. Synth. Catal. 353 (2011) 2885–2904.
[15] M. Guncheva, M. Dimitrov, D. Zhiryakova, Catal. Commun. 16 (2011) 205–209.
[16] M. Guncheva, M. Dimitrov, D. Zhiryakova, Process Biochem. 46 (2011) 2170–2177.
[17] A. David, N. Wang, V. Yang, A. Yang, J. Biotechnol. 125 (2006) 395–407.
[18] T. Terentyeva, A. Matras, W. Rossom, J. Hill, Q. Ji, K. Ariga, J. Mater. Chem. B 1 (2013) 3248–3256.
[19] A. Mayoral, R. Arenal, V. Gascón, C. Márquez-Álvarez, R. Blanco, I. Díaz, ChemCatChem 5 (2013) 903–909.
[20] R. Sanz, G. Calleja, A. Arencibia, E. Sanz-Pérez, Micropor. Mesopor. Mater. 158 (2012) 309–317.
[21] H. Yoshitake, T. Yokoi, T. Tatsumi, Chem. Mater. 14 (2002) 4603–4610.
[22] X. Wang, K. Lin, J. Chan, S. Cheng, J. Phys. Chem. B 109 (2005) 1763–1769.
[23] X. Wang, J. Chan, Y.-H. Tseng, S. Chen, Micropor. Mesopor. Mater. 95 (2006) 57–65.
[24] H. Ritter, D. Brühwiler, J. Phys. Chem. C 113 (2009) 10667–10674.
[25] Y. Shimada, M. Suenaga, A. Sugihara, S. Nakai, Y. Tominaga, J. Am. Oil Chem. Soc. 76 (1999) 189–193.
[26] P.A. Nunes, P. Pires-Cabral, M. Guillen, F. Valero, S. Ferreira-Dias, J. Am. Oil Chem. Soc. 89 (2012) 1287–1295.
[27] R. Jala, P. Hu, T. Yang, Y. Jiang, Y. Zheng, X. Xu, in: Georgina Sandoval (Ed.), Lipases and Phospholipases: Methods and Protocols, Methods in Molecular Biology, vol. 861, Springer Science + Business Media, New York, 2012, pp. 403–431.
[28] M. Haas, D. Bailey, W. Baker, T. Berka, D. Cichowicz, Z. Derewenda, R. Genuario, R. Joeger, R. Klein, K. Scott, D. Woolf, Fett/Lipid 101 (1999) 364–370.
[29] C. Gray, J. Narang, S. Barker, Enzyme Microb. Technol. 12 (1990) 800–807.
[30] M. Dimitrov, T. Tsoncheva, S. Shao, R. Köhn, Appl. Catal. B: Environ. 94 (2010) 158–165.
[31] C. Hammond, The diffraction of X-rays, in: The Basics of Crystallography and Diffraction, Oxford Science Publications, New York, 2001, pp. 203–242.
[32] E. Soto-Cantu, R. Cueto, J. Koch, P. Russo, Langmuir 28 (2012) 5562–5569.
[33] G. Chatel, C. Goux-Henry, A. Mirabaud, T. Rossi, N. Kardos, B. Andrioletti, M. Draye, J. Catal. 291 (2012) 127–132.
[34] B. Al-Duri, Y.P. Yong, J. Mol. Catal. B: Enzym. 3 (1997) 177–188.
[35] O.H. Lowry, N.J. Rosebrough, A.L. Farr, R.J. Randall, J. Biol. Chem. 193 (1951) 265–275.
[36] P. Halling, Biotechnol. Tech. 6 (1992) 271–276.
[37] A. Straathof, J. Jongejan, Enzyme Microb. Technol. 21 (1997) 559–571.
[38] M. Thommes, Chem. Ing. Tech. 82 (2010) 1059–1073.
[39] U. Derewenda, L. Swenson, Y. Wei, R. Green, P.M. Kobos, R. Joerger, M.J. Haas, Z.S. Derewenda, J. Lipid Res. 35 (1994) 524–534.
[40] J. Lewis, J. Am. Ceram. Soc. 83 (2000) 2341–2359.
[41] J. Palomo, C. Ortiz, M. Fuentes, G. Fernandez-Lorente, J. Guisan, R. Fernandez-Lafuente, J. Chromatogr. A 1038 (2004) 267–273.
[42] A. Mendes, R. Giordano, R. de, L.C. Giordano, H. de Castro, J. Mol. Catal. B: Enzym. 68 (2011) 109–115.
[43] L.N. de Lima, C. Aragon, C. Mateo, J. Palomo, R. Giordano, P. Tardioli, J. Guisan, G. Fernandez-Lorente, Process Biochem. 48 (2013) 118–123.
[44] D. Rodrigues, A. Mendes, M. Filice, R. Fernandez-Lafuente, J. Guisan, J. Palomo, J. Mol. Catal. B: Enzym. 58 (2009) 36–40.
[45] S. Hwang, K.-T. Lee, J.-W. Park, B.-R. Min, S. Haam, I.-S. Ahn, J.-K. Jung, Biochem. Eng. J. 17 (2004) 85–90.
[46] S. Pahujani, S. Kanwar, G. Chauhan, R. Gupta, Bioresour. Technol. 99 (2008) 2566–2570.
[47] S. Koshiro, K. Sonomoto, A. Tanaka, S. Fukui, J. Biotechnol. 2 (1985) 47–57.
[48] J. Kaar, A. Jesionowski, J. Berberich, R. Moulton, A. Russell, J. Am. Chem. Soc. 125 (2003) 4125–4131.
[49] Z. Yang, W. Pan, Enzyme Microb. Technol. 37 (2005) 19–28.
[50] S. Park, R. Kazlauskas, Curr. Opin. Biotech. 14 (2003) 432–437.
[51] F. Deive, A. Rodriguez, L. Rebelo, I. Marrucho, Sep. Purif. Technol. 97 (2012) 205–210.
[52] F. Deive, A. Rodriguez, A. Pereiro, J. Araujo, M. Longo, M. Coelho, J. Canongia Lopes, J. Esperanca, L. Rebelo, I. Marrucho, Green Chem. 13 (2011) 390–396.

[53] R. Lau, M. Sorgedragner, G. Carrea, F. van Rantwijk, F. Secundo, R. Sheldon, Green Chem. 6 (2004) 483–487.
[54] B. Liu, N. Wang, Zh Chen, Q. Wu, X. Lin, Bioorg. Med. Chem. Lett. 16 (2006) 3769–3771.
[55] M. Kidwai, R. Poddar, Catal. Lett. 124 (2008) 311–317.
[56] P. Vidya, A. Chadha, J. Mol. Catal. B: Enzym. 57 (2009) 145–148.
[57] A. Kurata, Y. Kitamura, Sh Irie, Sh Takemoto, Y. Akai, Y. Hirota, T. Fujita, K. Iwai, M. Furusawa, N. Kishimoto, J. Biotechnol. 148 (2010) 133–138.
[58] N. Galonde, K. Noh, G. Richard, A. Debuigne, F. Nicks, C. Jerome, M-L. Fauconner, Curr. Org. Chem. 17 (2013) 763–770.
[59] S. Mohile, M. Potdar, J. Harjani, S. Nara, M. Salunkhe, J. Mol. Catal. B: Enzym. 30 (2004) 185–188.
[60] R. Irimescu, K. Kato, J. Mol. Catal. B: Enzym. 30 (2004) 189–194.
[61] S. Bai, Z. Guo, W. Liu, Y. Sun, Food Chem. 96 (2006) 1–7.
[62] N. Kamiya, M. Goto, F. Nakashio, Biotechnol. Prog. 11 (1995) 270–275.